Environmental Science and Pollution Research (2022) 29:17132–17149
https://doi.org/10.1007/s11356-021-16922-8

RESEARCH ARTICLE

Temporal and spatial assessment of groundwater contamination with nitrate using nitrate pollution index (NPI), groundwater pollution index (GPI), and GIS (case study: Essaouira basin, Morocco)

Otman El Mountassir[1] · Mohammed Bahir[1,2] · Driss Ouazar[3] · Abdelghani Chehbouni[2,4] · Paula M. Carreira[5]

Received: 19 April 2021 / Accepted: 3 October 2021 / Published online: 17 October 2021

Abstract

Groundwater aquifers in Morocco's coastal regions are under serious threat as a result of climate change. This study was conducted to evaluate and map the quality of water resources, by evaluating the level of pollution of the groundwater in the Meskala-Ouazzi sub-basin, a coastal area of Essaouira based on the physico-chemical analysis of 58 samples using a geographic information system (GIS) technique, analytical analysis, nitrate pollution index (NPI), and groundwater pollution index (GPI). The diagram piper of the study area is dominated by Cl-Ca-Mg, Cl-Na, HCO_3-Ca-Mg, and SO_4-Ca types. The concentrations of nitrate ranged from 2 to 175 mg/L. It was discovered that 22% of the groundwater samples had nitrate amounts greater than the World Health Organization's recommended maximum allowable level of 50 mg/L. The NPI ranged between − 0.9 and 7.8. According to the classification of NPI, 44.8% of the total groundwater samples represent clean water, indicating that the groundwater in the study area is suitable for irrigation. GPI values ranging from 0.6 to 3.7, with an average of 1.7, identifies 37.9% of all groundwater samples as low polluted. The inverse distance weighting (IDW) approach was used to generate a spatial distribution map, which indicates that appropriate groundwater is present in the sub-upstream basin's part. Overall, the forte concentration in groundwater samples detected in western and central areas showed that the nitrate originated from large amounts of nitrogen fertilizer used by humans in agricultural activities during periods of irrigation. The low tritium (δ^3H) content shows that the aquifer recharge is stale water and excessive use of fertilizers leads to groundwater pollution faster over time.

Keywords Groundwater quality · Nitrate pollution index · Groundwater pollution index · Nitrate · Tritium · GIS

Introduction

Groundwater has become the main source of drinking, agriculture, and industry in most of the world's arid and semi-arid regions, particularly in coastal regions around the world (Bahir et al. 2014; Carreira et al. 2018; Trabelsi and Zouari 2019). The Meskala-Ouazi sub-basin is formed by carbonate rocks and is susceptible to anthropogenic nitrate intrusion due to aquifer leakage, especially when there is little or no soil (Bahir et al. 2014; Han and Jin 1996; Panno et al. 2001). In this context, several studies have evaluated the pollution of groundwater in coastal aquifers (Bahir et al. 2021a, 2021b; El Mountassir et al. 2020; Fenandes et al. 2005). On the other hand, a complete understanding of hydrogeochemical characteristics and their potential pollutions is essential for the regional groundwater sustainable use and protection (Bahir et al. 2021b; Bouaicha et al. 2019; Hamed et al. 2018; Kaid Rassou et al., 2005). Several pieces of research

Responsible Editor: Xianliang Yi

✉ Otman El Mountassir
otman.elmountassir@ced.uca.ma

[1] High Energy and Astrophysics Laboratory, Faculty of Sciences Semlalia, Cadi Ayyad University, Marrakech, Morocco

[2] Mohammed VI Polytechnic University (UM6P), IWRI, Ben Guerir, Morocco

[3] Mohammadia School of Engineers, Mohammed V University, Rabat, Morocco

[4] CESBIO, Université de Toulouse, CNRS, CNES, IRD, BPI 280, 31065 CEDEX 9 Toulouse, France

[5] Centro de Ciências E Tecnologias Nucleares, Universidade de Lisboa, C2TN/IST Lisbon, Portugal

such as (Bahir et al. 2021a, 2021b; Bahrami et al. 2020; El Mountassir et al. 2021a, 2021b; Kamaraj et al. 2021) have been carried out to determine the quality of the water and its hydrochemical properties. The deterioration of water quality generates significant health and environmental problems (WHO 2011). Nitrate (NO_3^-) is one of the major pollutants in the world's groundwater. The nitrate concentration in the groundwater above 10 mg/L can be toxic to infants and over time can cause stomach cancer (Wu and Sun 2016). According to the World Health Organization (WHO 2011), very rapid health problems can occur when drinking water rich in nitrates. The NO_3^- values greater than 50 mg/L in groundwater (WHO 2011) can be dangerous for human and animal life (Sall and Vanclooster 2009). High nitrate values can degrade water quality, causing eutrophication and the spread of toxic algal blooms in the water (Axinte et al. 2015, 2017; Ji et al. 2017). Moreover, a high concentration of nitrate in the groundwater can increase the risk of several diseases such as (a) methemoglobinemia, (b) diabetes, (c) spontaneous abortions, (d) cancer, (e) thyroid gland problems, (f) mutagenesis and (g) teratogenesis (Wu and Sun 2016). Therefore, the massive uses of fertilizers and pesticides, as well as the intensive cultivation of land, have contributed to the decrease and degradation of organic matter in the soil (Laftouhi et al. 2003). In addition, due to the absence of a special waste management system in the urban and rural areas, the random disposal of these wastes leads to negative environmental impacts on the soil and water (Nejatijahromi et al. 2019; Redwan et al. 2020; Wei et al. 2017). In the light of the extensive use of fertilizers and pesticides to obtain a good return in agriculture, it leads to a loss of the soil's ability to support agriculture and its erosion, which facilitates nitrate leakage into the groundwater (Filintas 2005; Mtoni et al. 2013). The presence of elevated nitrate levels in groundwater correlates with urbanization and cultural activities, where there is a discharge of wastewater that is not treated before discharging to the environment. Overexploitation of groundwater due to rapid urbanization in the center of the study area accelerates the deterioration of the quality of groundwater. However, the results obtained could be a basis for regional decision-makers for better management, planning, and protection of this resource. Furthermore, this work was done to systematically study nitrate pollution in the Meskala-Ouazzi sub-basin, including the distribution of nitrate concentrations in the study area with the identification of the most concentrated areas and the exact cause of their rise. Therefore, it is important to fully understand the sources and variability of the nitrate concentration in the groundwater of coastal aquifers in order to manage water resources well. The main objectives of this work are (a) to study the spatial distribution of the main ions in groundwater, (b) to identify the origin of groundwater, (c) to determine the dominant geochemical processes and factors that control the hydrogeochemical characteristics of Meskala-Ouazzi sub-basin, (d) compare nitrate levels to WHO standard values, and (e) spatial distribution of nitrate concentration in coastal areas using two NPI and GPI methods.

Study area and methodology

Geographical and climatic setting

The region studied corresponds to the syncline of Bouabout, located about 70 km east of the city of Essaouira (Fig. 1). It is part of the large basin of South West Morocco (Duffaud 1960). It is an area with a semi-arid climate where the average rainfall does not exceed 300 mm/year (El Mountassir et al. 2020) and varies greatly from year to year. Winter is mild and humid, but summer is hot and dry. The temperature is moderate (19 °C on average), with a significant thermal difference. This basin occupies a total surface of 1196 km^2.

Geology and hydrogeology

In the Meskala-Ouazzi sub-basin, the structure is made up of two major aquifers. The Plio-Quaternary aquifer, which is mostly made up of sand, sandstone, and conglomerates, contains the majority of the water supply. Calco-dolomitic aquifers dominate the Cenomanian–Turonian aquifer. Groundwater is one of the main water resources for both drinking water supply and irrigation (Bahir et al. 2000). The combination of tectonic and diapirism effects has caused the compartmentalization of the Essaouira basin into several aquifer systems whose hydraulic relationships are difficult to understand (Mennani 2001a). They correspond more or less to synclinal basins. The Bouabout sub-basin contains most of the water resources of the region and is crossed by the oued lgrounzar which collects the water (El Mountassir et al. 2020). Its perennial flow regime is due to a set of springs that drain different carbonate levels (Mennani 2001a). However, the Cenomano-Turonian aquifer remains the most important because of its lithological (limestones and dolomites alternating with marls) and structural characteristics (important fracturing). Its wall is constituted by the gray marls of the Lower Cenomanian (El Mountassir et al. 2020). Given its geological and fracture properties, the Cenomanian, Turonian, and Senonian layers must be considered as a multilayer aquifer with "permeability to rupture" (Castany 1982). The Cenomanian aquifer is subdivided by two non-homogeneous zones: (a) the lower aquifer is of fissure or karstic type. It gives rise in the lowest areas to springs with different flows and the upstream part is characterized by the Cenomanian formed of limestone marls and marls, with a thickness of 200 m is characterized by very low

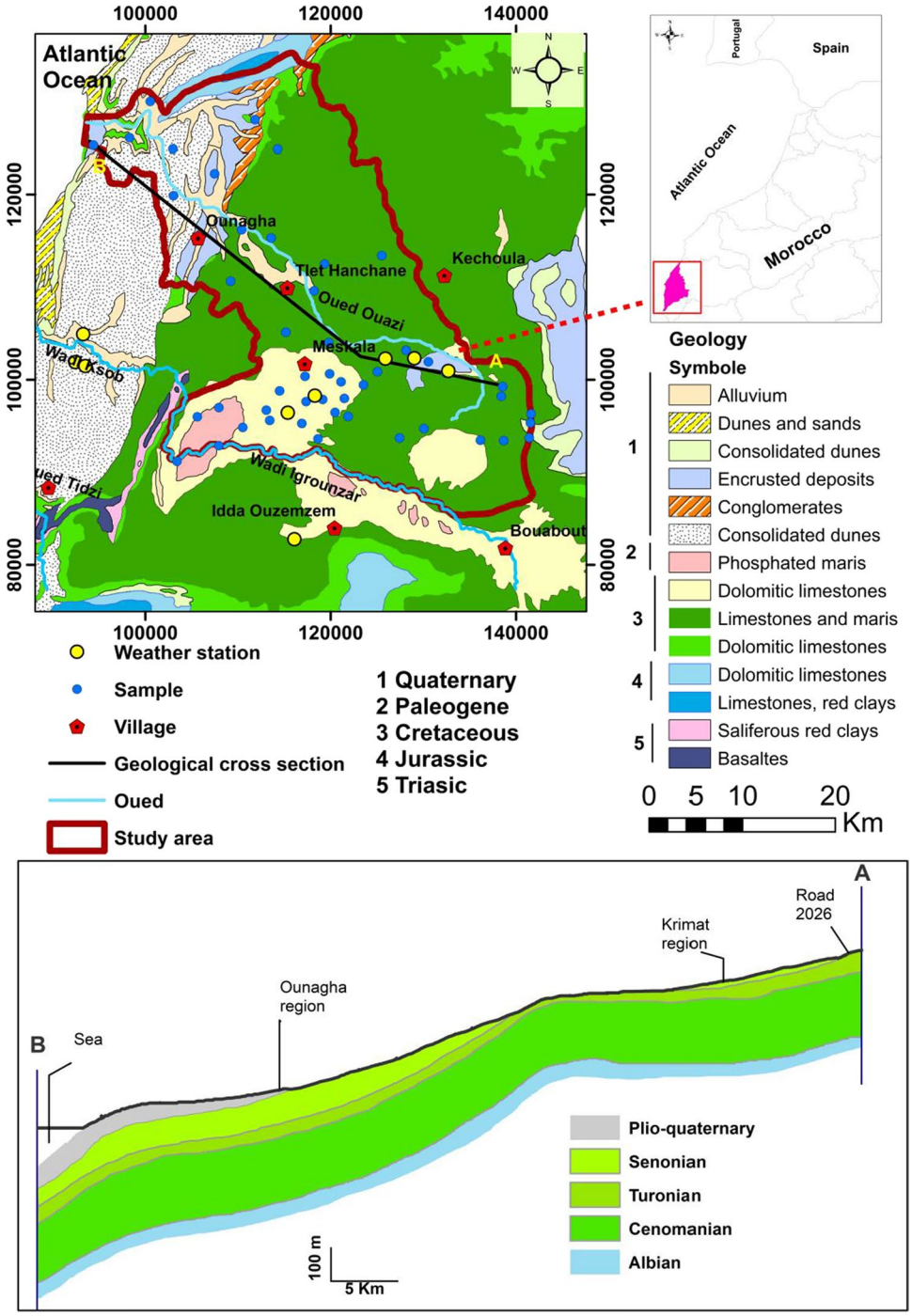

Fig. 1 Geographic situation, location of groundwater sampled points in Meskala-Ouazi sub-basin, geological, and cross section of the study area

permeability and (b) the Upper part of Cenomanian formed of yellow limestones and marly limestones, Therefore, the thickness of this aquifer is about 200 m (Bahir et al. 2000). The Turonian aquifer is relatively more homogeneous than the Cenomanian and is characterized by dolomitic limestone and beige limestone, with marly yellow limestone detritus and flammable limestone in Fig. 1. The average thickness of this aquifer is 50 m (Bahir et al. 2000).

Sampling and methods

During the year 2019, 58 groundwater samples were obtained along the Meskala-Ouazzi sub-basin. The groundwater samples were collected in springs, dug wells, and boreholes issuing from the coast to the Wadi Ouazi and Wadi Igrounzar in Fig. 1. The temperature (T °C), pH, and electrical conductivity (EC) were measured in situ using

portable Hanna meters (HI9828). A piezometric probe (range 200 m) was used to determine the depth of the water table. The crops in the study area are mainly wheat, olive, carob, and argan. The field sampling was carried out during March 2019 using 116 pre-cleaned polyethylene plastic bottles. The bottles were washed twice with the sampled water before filling after pumping out water from the wells for around 1–3 min to clear any residual water in the well. With the representative samples, it excludes any external contamination. Analyses of elements (Na^+, SO_4^{2-}, K^+, Ca^{2+}, Mg^{2+}, Cl^-) was carried out at the Geosciences and Environment Laboratory of the Ecole Normale Supérieure (ENS) (Cadi Ayad University, Morocco). Alkalinity (as HCO_3^-) was determined by using the titration method with HCL within 12 h after sampling (Appelo and Postma, 2014). The two parameters Na^+ and K^+ were performed using inverse liquid chromatography (ILC) in the University Center for Analysis, Technology Transfer & Incubation Expertise (CUAE2TI) at "Faculty of Sciences" (Ibn tofail University, Morocco). In addition, the charge balances and uncertainties of all samples measured cation and anion concentrations were within ± 5%. All the isotopic determinations were performed at C^2TN/IST (Portugal) laboratories of the Universidade de Lisboa, using the mass spectrometer SIRA 10 VG-ISOGAS for δ^2H and $\delta^{18}O$ determinations. Electrolytic enrichment was used to determine the tritium (^3H) content of the 2016 campaign, followed by a liquid scintillation counting process (Lucas and Unterweger 2000).

Analytical methods

Principal component analysis (PCA), correspondence analysis (CA), and discriminant analysis are common approaches for solving multivariate problems (Yuan et al. 2017), which seek to summarize results from many variables thus reducing information loss. These methods have also been used in hydrology, geology, meteorology, environmental science, industry, agriculture, and medicine (Angers et al. 1999; Obeidat et al. 2007; Redwan et al. 2020). In the present Meskala-Ouazzi sub-basin analysis, PCA and CA were used to analyze hydrogeochemical data. PCA is a data transformation technique that exposes a basic underlying structure within a multivariate dataset, while CA is a data grouping technique that classes samples or indices with identical characteristics (Wu et al. 2014). The XLSTAT-Pro software was used to process the analytical results. Accordingly, reports of major ionic and stoichiometric analyses were used to determine the interrelationships of the various major elements to better explain and demonstrate the hydrogeochemical processes in groundwater, as well as to confirm the results of the correspondence analysis. A qualitative analysis, such as the distribution of nitrate in the Meskala-Ouazzi sub-basin, was carried out to study the pollutant transport mechanism and possible routes, and some potential factors, such as groundwater depth, were also studied, which are considered to be significant factors affecting the transit contaminants in the groundwater of the Meskala-Ouazzi sub-basin.

Nitrate pollution index

For the calculation of nitrate contamination, a single parameter water quality index called the nitrate pollution index (NPI) was used. The NPI index indicates that human activity has contributed to nitrate pollution in groundwater. The following formula (1) (Obeidat et al. 2012) was used to determine the NPI:

$$NPI = \frac{\left(C_s - HAV\right)}{HAV} \quad (1)$$

where C_s is the nitrate concentration of each sample and the threshold value for anthropogenic origin is called HAV (value affected by humans), according to Obeidat et al. (2012) taken HAV at 20 mg/L. Water quality was graded into five groups based on the nitrate pollution index (NPI) results, as seen in Table 1.

Groundwater pollution index (GPI)

Subba Rao (2012) developed the groundwater pollution index (GPI). It usually assesses the relative impact of individual chemical variables such as TDS (total dissolved solids), pH, TH (total hardness), Mg^{2+} (magnesium), Cl^- (chloride), Na^+ (sodium), Ca^{2+} (calcium), K^+ (potassium), NO_3^- (nitrate), HCO_3^- (bicarbonate), and SO_4^{2-} (sulfate), on the general quality of drinking water from Meskala-Ouazzi

Table 1 Values and categories of NPI and WHO limits on NO_3^- (WHO 2011; Obeidat et al. 2012)

NPI value	NPI interpretation	NPI class	NO_3^- (mg/L)	WHO standard	NO_3^- Class
< 0	Clean (unpolluted)	1	< 50	Desirable limit (DL)	1
0–1	Light pollution	2	50	Maximum permissible limit (MPL)	2
1–2	Moderate pollution	3	> 50	Not permissible limit (NPL)	3
2–3	Significant pollution	4			
> 3	Very significant pollution	5			

sub-basin. The GPI is calculated according to a general method developed by Subba Rao (2012), which is as follows:

Step one

Each chemical parameter is given a relative weight (RW) ranging from one to five, based on its relative effect on the overall content of drinking water. The maximum RW "five" is applied to parameters that have the most significant effects (SO_4^{2-}; Cl^-; and NO_3^-), and parameters with less effect are given a minimum RW "one" such as HCO_3^- and K^+. Furthermore, RW "fourth" has been allocated to pH, Na^+, TH, and TDS, and finally the minimum value "two" is assigned to Mg^{2+} and Ca^{2+} (Table 2).

Step two

The weight parameter (WP) is defined as the ratio of each physical–chemical parameters, RW divided by the total number of all relative weights. The corresponding equation is used to calculate the WP (Eq. (2))

$$WP = \frac{RW}{\sum RW} \tag{2}$$

Step third

By dividing the concentration of chemical element C_i in each groundwater sample by the respective recommendations for drinking water quality (WHO 2011), the state of concentration (SOC) is determined by the following formula (Eq. (3)):

$$SOC = \frac{C_i^n}{\mathcal{QWQS}} \tag{3}$$

Step fourth

The following equation (Eq. (4)) is used to calculate the average groundwater content (OQG) for consumption

$$OQG = WP \times SOC \tag{4}$$

WP indicates the weight parameter and SOC indicates the concentration status.

Step five

The GPI is calculated by adding all OQG values together (Eq. (5)) to determine the impact of pollutants on groundwater quality:

$$PIG = \sum OQG \tag{5}$$

Subba Rao (2012) is classified GPI into 5 main categories, i.e., insignificant pollution (GPI less than one); second low pollution (GPI: between1 and 1.5); third moderate pollution (GPI: ranging from 1.5 to 2); fourth high pollution (GPI: ranging between 2 and 2.5); and finally the last category is very high pollution (GPI above 2.5) (Kamaraj et al. 2021; Subba Rao 2012).

Table 2 Relative weight (RW), weight parameters (WP), and drinking water quality standards (WHO 2011)

Chemical parameters	Relative weight (RW)	Weight parameter (WP)	Drinking water quality standards (DWQS)
pH	4	0.108	7.5
TDS (mg/L)	4	0.108	500
TH (mg/L)	4	0.108	300
Ca^{2+} (mg/L)	2	0.054	75
Mg^{2+} (mg/L)	2	0.054	30
Na^+ (mg/L)	4	0.108	200
K^+ (mg/L)	1	0.027	12
HCO_3^- (mg/L)	1	0.027	300
Cl^- (mg/L)	5	0.135	250
SO_4^{2-} (mg/L)	5	0.135	200
NO_3^- (mg/L)	5	0.135	50
Sum	37	1	

Geostatistical modeling

GIS applications are useful tools for determining the spatial distribution of groundwater quality characteristics by combining spatial data with other information that will assist environmental protection and resource planning (Assaf and Saadeh 2009; Bouteraa et al. 2019), also for the use of geostatistics in the evaluation of groundwater quality (Barkat et al. 2021). Furthermore, geostatistics is a mathematical tool concerned with spatial correlation schemes and the variogram, a quantitative spatial correlation measure commonly used in geostatistics (Seo et al. 2015). The geostatistical interpolation technique is a powerful approach with the ability to reliably estimate and present the spatial distribution from point data (Assaf and Saadeh 2009). Meanwhile, interpolation techniques such as Kriging will provide a neutral, best linear approximation of a regionalized vector in non-sampled locations (Mei et al. 2014; Venkatramanan et al. 2016).

One of the main advantages of kriging is that it presents the interpolation error of the values of the regionalized variable where there are no initial measurements (Karami et al. 2018). This feature provides a measure of the spatial distribution of the variable's estimation accuracy and reliability (Barkat et al. 2021). The spatial variability of a regionalized variable is described by a semi-variogram.

The semi-variogram should be determined from the regionalized variables data, prior to kriging estimation, as illustrated in Eq. (6), which is a graphical representation of the mean square variability between two contiguous locations distanced by h. The experimental variogram ($\gamma(h)$) is defined as a separation distance of h, which is the half

average squared difference between the value at $Z(x_i)$ and the value at $Z(x_i+h)$ (Lark 2000):

$$\gamma(h) = \frac{1}{2n(h)} \sum_{i=1}^{n(h)} \left[Z(x_i) - Z(x_i+h)\right]^2 \quad (6)$$

where $Z(x_i)$ is the value of the variable Z at the location of x_i, h is the lag, and $n(h)$ is the number of pairs of sample points separated by h. The geostatistical analysis was performed using ArcGIS 10.2 software for generating spatial distribution maps.

Results and discussion

Hydrochemistry

Table 3 summarizes the statistical study of physiochemical parameters of 58 groundwater samples. The pH values of groundwater samples in the research region ranged from 7 to 8.4, which were neutral to significantly alkaline (Table 3). The TDS values in the Meskala-Ouazzi sub-basin ranged from 308 to 2867 mg/L (Table 3), which were all well within the 1000 mg/L cap set by the Standards for Drinking Water Quality (WHO 2011). Furthermore, chloride (Cl^-) was the most abundant anion in all 58 groundwater samples, followed by bicarbonate (HCO_3^-). The dominant cation was calcium (Ca^{2+}), followed by the parameter magnesium (Mg^{2+}). These results demonstrated that Ca^{2+}, Mg^{2+}, Cl^-, and HCO_3^- were the dominant ions in this region (Meskala-Ouazzi sub-basin). Therefore, the projection of the representative groundwater samples on this diagram piper shows that the most dominant chemical is Cl-Ca-Mg following by Cl-Na water type (Fig. 2).

Relationships among major ions

Figure. 3A revealed that dolomite and calcite dissolution was not the only source of calcium (Ca^{2+}) and magnesium (Mg^{2+}) in groundwater, which is supported by the correlation factor ($R^2=0.26$). Similarly, the HCO_3^- is not strongly correlated either with Ca^{2+} (Fig. 3B), pointing to a different origin, other than calcite dissolution. In addition, it has been proposed that another cause, such as the dissolution of gypsum minerals or the exchange of cations between Ca^{2+} and Na^+ could be responsible for the excess of Ca^{2+}.

Groundwater samples collected in the Meskala-Ouazzi sub-basin are characterized by the precipitation of calcite (El Mountassir et al. 2020). The correlation between Ca^{2+} versus SO_4^{2-} diagram (Fig. 3C) shows a moderate correlation with ($R^2=0.66$), and the maximum of the sample area's points are aligned on a line with a slope of 1:1, reflecting gypsum and/or anhydrite dissolution. Therefore, the points below the line of slope (1:1) formed by the mineralized waters of the upstream part and display an excess Ca^{2+} which might be due to a base-exchange mechanism.

The Figure 3D shows a strong correlation between the Na^+ and the Cl^- concentration ($R^2=0.81$) which were obtained for the groundwater samples. However, this finding reveals that certain points are placed on the slope (1:1), implying that halite dissolution is involved in the Meskala-Ouazzi sub-basin groundwater salinization. As a result, high Cl^- relative to Na^+ values is observed downstream of the Meskala-Ouazzi sub-basin, along the Atlantic Ocean, indicating that seawater penetration is possibly affecting groundwater mineralization (Bahir et al. 2018)

Cation exchange is a crucial hydrochemical mechanism that has a significant impact on the evolution of groundwater's hydrochemical characteristics (Carreira et al. 2018). The ratio $[(Ca^{2+}+Mg^{2+})\ (SO_4^{2-}+HCO_3^-)]$ and (Na^++Cl^-) is commonly used to assess the effect of cation exchange in the Cenemano-Turonien aquifer (Yuan et al. 2017). In the present case, a slope of −0.62 (Fig. 4A) is seen which indicates that Na^+, Ca^{2+}, and Mg^+ participate in the ion exchange process and are derived from interaction with the Cenemano-Turonien aquifer. The majority of groundwater samples were near to slope 1:1, as seen in Fig. 4B, indicating that cation exchange is a significant factor influencing the hydrochemical composition of groundwater.

A plot of $SO_4^{2-}+HCO_3^-$ vs $Ca^{2+}+Mg^{2+}$ (Fig. 4B) was examined to ascertain the presence of silicate weathering and reverse ion exchange. The dominance of $SO_4^{2-}+HCO_3^-$ over $Ca^{2+}+Mg^{2+}$ is an indicator of silicate weathering, whereas the abundance of $Ca^{2+}+Mg^{2+}$ is an indicator of reverse ion exchange (Elango and Kannan 2007); however, in the present study, all samples show a dominance of $Ca^{2+}+Mg^{2+}$ over SO_4^{2-} and HCO_3^- with a strong correlation with ($R^2=0.83$). The cation exchange phenomenon, which is added to the dissolution mechanism and the marine impact, controls the groundwater mineralization of the Cenemano-Turonien aquifer in general, according to this diagram.

Water pollution analysis

Figure 5A shows the effects of the correspondence analysis (CA) using the factor load matrix (Table 4), with F1 and F2 represent the key factor loads of the parameters and variables, respectively. Correspondence analysis is a simple method that makes it possible to study the association between qualitative variables (physico-chemical parameters) and quantitative variables (groundwater samples). The first axis of the major factor (F1) played a vital role in analyzing groundwater quality in the Meskala-Ouazzi sub-basin. Additionally, the second major factor axis (F2) can also evaluate water quality with a lower effect than F1 of all groundwater

Table 3 Physico-chemical composition of the samples analyzed from the Meskala-Ouazi sub-basin

Sample	pH	T °C	TDS mg/L	EC µS/cm	Ca^{2+} meq/L	Mg^{2+}	Na^{+}	K^{+}	HCO_3^{-}	Cl^{-}	SO_4^{2-}	NO_3^{-}	IB
S1	7.44	21.48	2266	4530	14.64	18.9	17.2	1.1	8.2	34.0	19.7	0.5	−9.2
S2	7.5	19.21	1059	2128	6.96	8.6	7.9	0.5	9.8	16.4	0.3	0.1	−5.3
S3	7.82	18.02	1125	2249	7.6	7.9	8.6	0.3	6.1	16	5.6	1	−8.1
S4	7.45	19.71	2105	4200	2.16	2.8	29.2	0.3	5.8	33.2	0.9	0.5	−8
S5	7.13	21.71	1090	2179	9.4	11.6	5.5	0.2	9.4	18.0	2	0.9	−6.1
S6	8.38	17.8	308	615	4.1	3.4	1.4	0.1	4.0	5.2	0.8	0.1	−5.7
S7	7.71	20.75	1190	2381	9.04	8.4	5.7	0.2	9.8	13.2	4.8	0.2	−9
S8	7.45	20.18	1924	3842	18.24	8.2	9.8	0.4	7	18.2	16.9	0.2	−7.2
S9	7.55	20.27	1099	2199	13.12	7.4	6.9	0.2	5.9	15.2	5.9	0.1	0.9
S10	7.2	23.63	538	1075	5.92	7.9	1.2	0.1	8	9.2	0.4	0.3	−8.6
S11	7.21	24	486	972	5.12	5.1	6.7	0.1	8	6	0.6	1.7	1.9
S12	7.51	22	946	1888	6.72	8.1	5.2	0.1	7	12.8	2.3	0.5	−5.7
S13	7.45	21.06	2192	4380	21.5	6.2	17.2	0.3	8.6	38.1	3.7	1.9	−7.4
S14	7.66	21.35	1259	2500	7.5	7.7	12.7	0.4	7.8	24	0.3	0.1	−6.4
S15	7.6	20.9	1515	3016	8.4	6	12.4	0.5	8	19.2	2	2.6	−7.7
S16	7.78	19.96	368	736	7	4.6	0.8	0.0	4.8	5.3	0.7	0.4	5.2
S17	7.55	18.91	441	882	9	7.3	0.6	0.1	9	6.8	1.2	0.3	−0.8
S18	7.76	20.95	398	796	5.2	6.6	0.5	0.0	8.2	5.2	0.3	0.2	−5.9
S19	7.45	21.44	753	1510	8	9.1	3.5	0.1	8	11.6	3.1	0.3	−5.4
S20	7.42	20.8	778	1559	6.6	7.9	3.6	0.1	7	13.2	1.7	0.2	−9.7
S21	7.81	19.6	1061	2123	13.2	11.5	5.7	0.1	11.8	17.6	1.6	0.2	−1.2
S22	7.08	19.45	1848	3690	12.88	13.6	13.0	0.1	9.4	32.4	3.7	1.4	−8.4
S23	7.16	20.3	2867	5738	24.16	8.4	23.5	0.3	9.2	51.3	5.6	1.1	−8.8
S24	7.78	21.26	510	1020	5.6	6.7	1.9	0.1	8	6.4	1.5	0.3	−6.4
S25	7.76	19.3	668	1336	6.8	7.8	2.8	0.3	7.2	8.4	5.5	0.3	−9.3
S26	7.99	18	1374	2750	13.44	13.8	4.3	0.3	6.2	12.8	17	1	−7.6
S27	7.47	21.4	704	1411	6.72	8.3	3.3	0.1	8.2	7.6	5.3	0.2	−7.6
S28	7.4	19.63	793	1584	7.84	9.1	4.4	0.1	7.8	8.8	8.7	0.1	−8.4
S29	7.3	18.8	1088	2173	11.6	12.9	3.9	0.1	9.2	8	12.4	0.6	−2.8
S30	7.98	14.85	922	1843	7.28	7.5	4.3	0.6	7.8	11.6	1.6	1.3	−6.2
S31	7.08	16.5	787	1574	5.12	7.5	3.5	0.1	6.7	8.5	2.7	0.5	−6.1
S32	7.57	20.3	972	1543	9.12	14.5	4.2	0.4	7.1	10.4	8.0	0.2	4.6
S33	7.09	17.25	1824	3646	38.4	9	2.4	0.3	8.8	9.6	40.4	0.2	−8.2
S34	7.59	18.04	1710	3389	21	21.4	6.6	0.3	11.2	18.8	27	0.7	−7.8
S35	7.53	17.5	596	1192	6.72	5.5	3.5	0.1	6.2	8.8	2.2	0.2	−4.8
S36	7.2	22.15	631	1261	6.24	8	2.4	0.1	6.6	8.4	4.5	0.4	−8.5
S37	7.8	21.03	431	862	4.4	2.6	2.5	0	5	3.2	0.6	0.5	1.4
S38	7.24	20.5	2487	4965	15.6	24.5	15.2	0.2	10.4	26.4	24.4	2.8	−7.2
S39	7.53	20.65	1045	2087	6.24	6.7	9.3	0.6	6.9	14.8	3.3	0.3	−5
S40	7.01	22.83	1474	2939	27.5	10.7	2.2	0.2	10.4	8.8	29.4	0	−9.1
S41	7.17	21.02	1076	2149	9.6	10.8	5.7	0.1	11.8	11.2	6.6	0.3	−6.7
S42	7.65	22.05	1221	2440	9.5	12	5	0.9	14.7	13.6	3.6	0.1	−8
S43	7.4	22.9	1612	3220	13.04	13.8	13.3	0.2	9.8	26.8	6.8	0.6	−4.5
S44	7.56	20.96	1116	2230	6.48	3.2	9.1	0.1	6.9	12.5	1.9	0.2	−6.5
S45	7.56	21.45	1130	2266	6.16	6.7	8.3	0.1	6.9	13.6	3.9	0.4	−7.8
S46	7.22	20.68	2143	4277	12.32	6.1	16.9	4.3	7.4	31.2	3.3	2.7	−6
S47	7.28	20.8	1329	2657	8.32	11.1	8.1	0.1	7	19.2	6	0.7	−8.9
S48	7.08	23	1404	2804	10.08	12.8	8	0.1	9.6	18.8	7.8	0.6	−8.5
S49	7.35	21.7	1104	2203	9.4	9.3	5.7	0.2	8.4	13.6	5.8	0.7	−7.4
S50	7.3	19.15	2100	4216	21	24.4	7.8	0.3	9.6	18.8	34.7	0.1	−8.3

Table 3 (continued)

Sample	pH	T °C	TDS mg/L	EC µS/cm	Ca^{2+} meq/L	Mg^{2+}	Na^{+}	K^{+}	HCO_3^{-}	Cl^{-}	SO_4^{2-}	NO_3^{-}	IB
S51	7.27	20.8	2179	4349	9.8	15.1	19.7	0.2	8.2	36.7	8.2	1	−9.3
S52	7.43	20.8	1646	3286	14	9.7	9.5	1.6	6.6	26.8	6.1	1.1	−7.8
S53	7.38	20.95	1070	2140	5.4	7.4	8.4	0.1	8.6	13.2	2.2	0.5	−7
S54	7.18	22.2	1140	2277	9.2	7.2	7.9	0.3	10.8	16	2.1	0	−8
S55	7.5	22.7	1076	2148	7.7	10.1	6.3	0.1	8.4	15.2	3.9	0.4	−6.9
S56	7.32	21.5	1327	2650	10.5	10.1	7.0	0.1	7.8	19.6	4.9	0.2	−7.9
S57	7.4	20.8	940	1873	5.8	3.8	8.1	0.1	5.3	12.4	2.3	0.5	−7.3
S58	7.4	19.2	2190	4370	15.7	21	12.1	2.2	9.8	33.2	14.3	0.4	−6.2
Min	7	14.9	308	615	2.2	2.6	0.5	0	4	3.2	0.3	0	−9.7
Max	8.4	24.0	2867	5738	38.4	24.5	29.2	4.3	14.7	51.3	40.4	2.8	5.2
Mean	7.5	20.5	1231.6	2453.8	10.5	9.6	7.6	0.4	8.1	16.5	6.9	0.6	−6.2

*IB, ionic balance

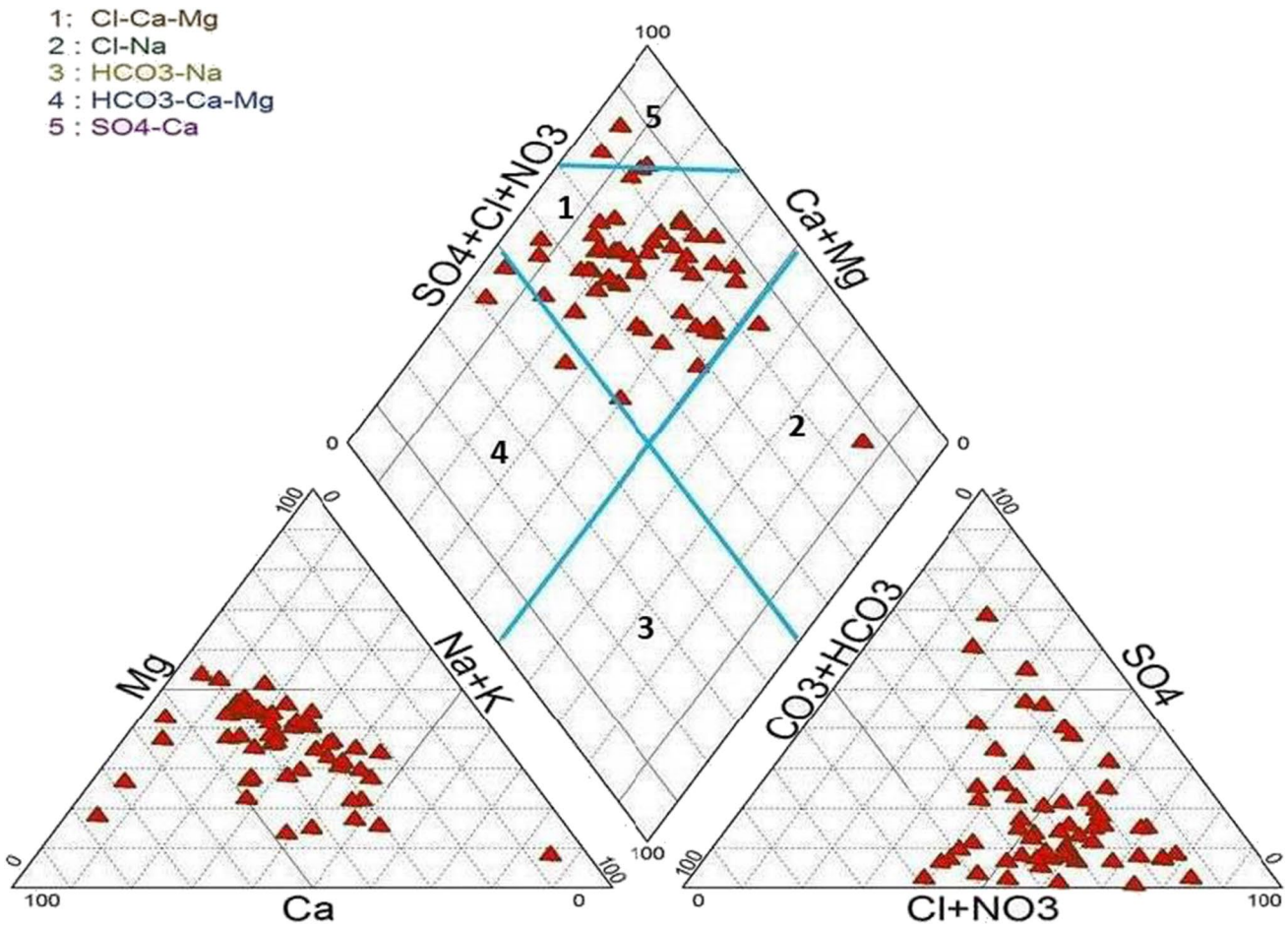

Fig. 2 Piper diagram of analyzed groundwater samples

samples. The first two PCs, 22.71% and 56.88%, covered more than 77% of the total variance in all data of the study area. Table 4 shows that SO_4^{2-} and HCO_3^{-} had the highest absolute values of F1 and F2, respectively, and were thus considered to be the primary water quality indicators. TDS were found in the middle of the F1 and F2 axes, with lower factor loads, indicating that it is not a factor influencing water pollution in the study region. Na^{+} and Cl^{-} were

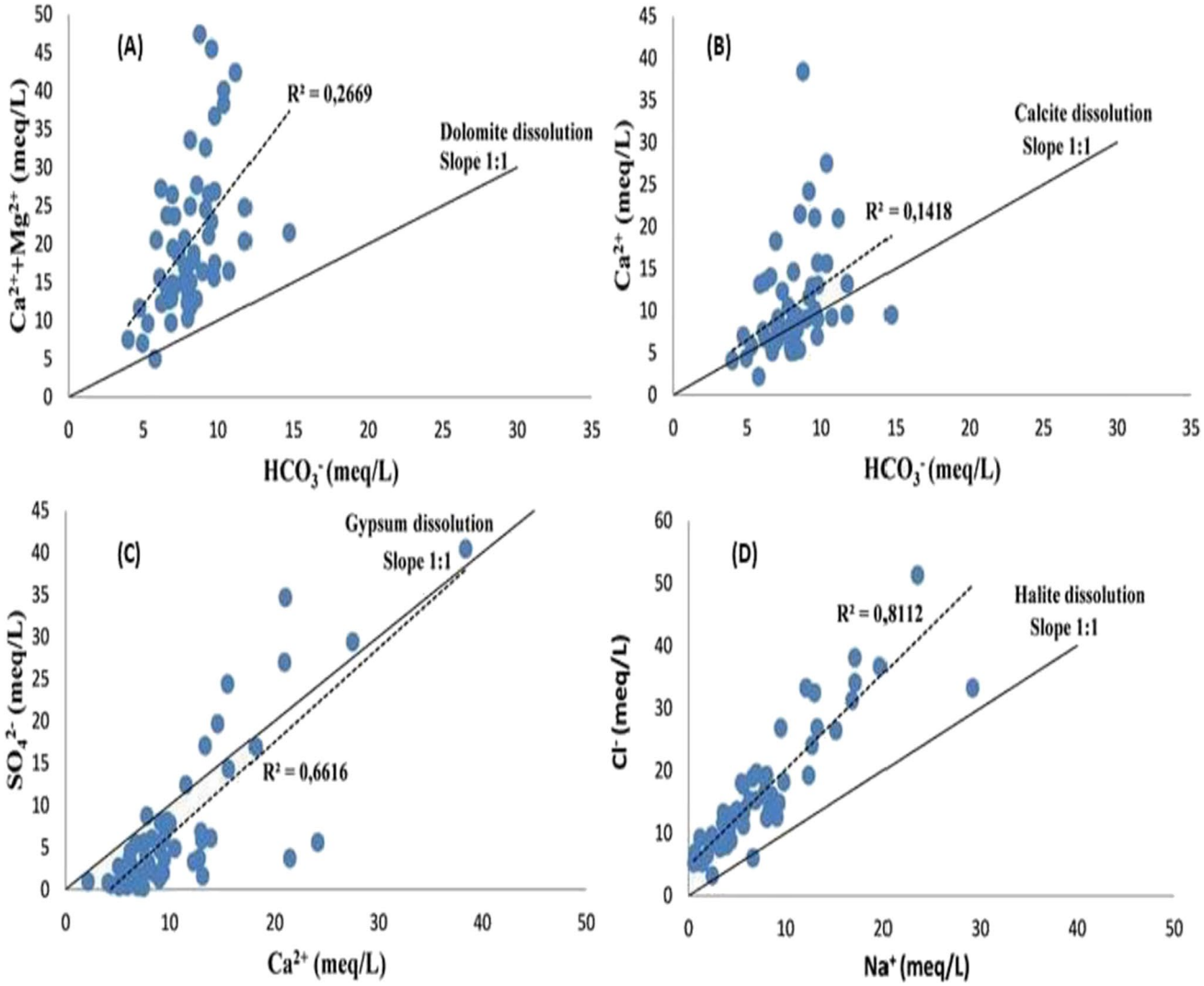

Fig. 3 Water–rock interaction in Meskala-Ouazzi groundwater samples: **A** Ca^{2+} + Mg^{2+} vs HCO_3^- plot; **B** Ca^{2+} versus HCO_3^- plot; **C** SO_4^{2-} versus Ca^{2+} plot; and **D** Cl^- versus Na^+ plot

located in the positive part of the F2 axis, also indicating the strong correlation between them, and this translated by the effect of the marine intrusion (Bahir et al. 2018) in the study area of the Meskala-Ouazzi sub-basin.

Figure 5A indicates some useful information to determine the source of pollution, and this is indicated by the distribution between the chemical parameters (variable) and the 58 groundwater. The origin will be the same for parameters that are in the same direction as axes F1 even F2 or whether the variables are very similar. The variables Cl^-, NO_3^-, Na^+, and K^+ were located in the same line (direction) of the F2 axis, indicating a similar source. The factors NO_3^- and Cl^- correspond to the main ions in nitrogen fertilizers, which include ammonium chloride (NH_4Cl), ammonium nitrate (NH_4NO_3), and others (Mekala et al. 2017). In the study area, there is almost no soil in the Essaouira region, so it is difficult to keep NH_4^+ ions at the top of the soil profile, some ions are absorbed by crops and soil roots, and the rest is usually converted to NO_3^- by nitrification and entering the aquifer (Mekala et al. 2017), as shown in Fig. 5B. As a result, it is possible that NO_3^- pollution is related to agricultural practices.

Carbon, hydrogen, oxygen, nitrogen, potassium, phosphorus, calcium, magnesium, sulfur, iron, manganese, zinc, copper, chlorine, molybdenum, and boron are all important nutrients that plants use to complete their growth cycle. Morocco used 3 essential elements in agriculture in the majority of soils which are potassium (K), phosphorus (P), and nitrogen (N). Therefore, the origin of potassium comes from deposits, underground, or marine, and from mixtures of KCl and NaCl (Brindha et al. 2014). These minerals are either dissolved in water or extracted as solids for their

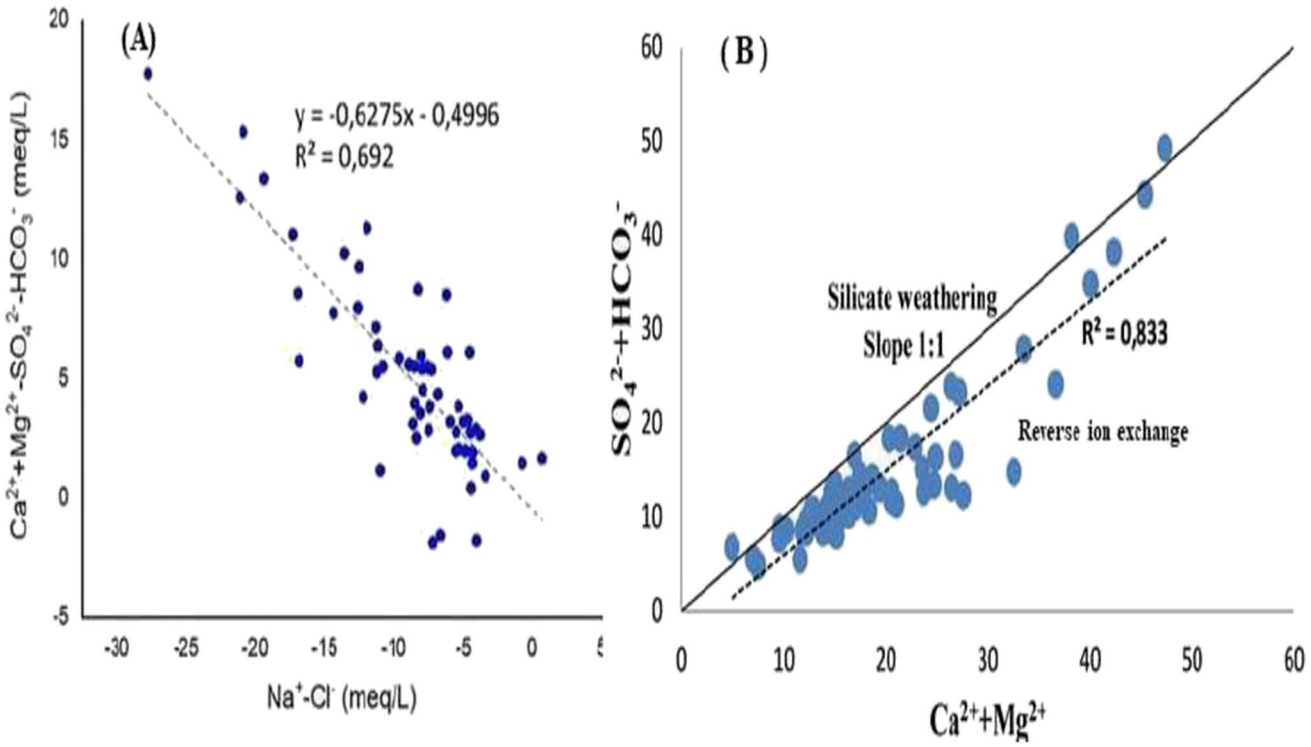

Fig. 4 **A** $Ca^{2+} + Mg^{2+}$-SO_4^{2-}-HCO_3^- vs Na^+-Cl^- plot, **B** $SO_4^{2-} + HCO_3^-$ vs $Ca^{2+} + Mg^{2+}$ plot

extraction. When fertilizer is brought to the soil, it undergoes chemical and biological transformations which eventually release into the soil solution (certain soil moisture is necessary), depending on its composition, nitrogen in the form of NO_3^- and/or NH_4^+, phosphorus in the form of $H_2PO_4^-$ or HPO_4^{2-} and potassium in the form of K^+ (Brindha et al. 2014). These nutrients can either be absorbed by the roots of plants, accumulate in the soil, or be lost through various processes (Mekala et al. 2017). In the soil, potassium fertilizers release K^+ which can be absorbed by plants when necessary or fixed by soil colloids and thus become stored for later use (Brindha et al. 2014).

In particular, all groundwater samples that are covered by coastal areas exposed to agricultural activity have not been contaminated with nitrates or have been contaminated to the same level, but there are other possible reasons such as the tourist side located near the sea and several other reasons will be discussed in the following paragraphs. Significant factors in determining the nitrate content in the Meskala-Ouazzi sub-basin include the concentration of nitrates, the movement of moisture in the sediments (flow), and the thickness of the unsaturated zone. Following the absence of a sewerage network in our studies, the Cl^- is playing a very important role in the determination of the contamination of groundwater by wastewater because it does not depend on microbiological and physical processes, in the end chemical (Fig. 5C) (Redwan et al. 2020; Wei et al. 2017). As a result, Cl^- from chemical fertilizers is often associated with increased NO_3^- concentrations (Wei et al. 2017), whereas higher Cl^- concentration sources in groundwater. In the study area, the groundwater samples with a high Cl^- content and a low NO_3^-/Cl^- ratio were mainly polluted by wastewater from the treatment plant or by livestock effluents. The highest ratios were around the treatment plant. Groundwater samples containing high concentrations of NO_3^- and Cl^- may be linked to agricultural inputs (Fig. 5C). The depth of the groundwater varied from a few meters to several meters, with most groundwater samples falling between 4.8 and 50.3 m, indicating the thickness of unsaturated areas.

Figure 5D indicates the concentrations of NO_3^- as a characteristic of groundwater levels for the majority of groundwater; it can be inferred that there was virtually no association between nitrate concentrations and groundwater levels for all groundwater samples in the Meskala-Ouazzi sub-basin, because of the average slow nitrate rate in the unsaturated area, according to Wei et al. (2017), changes in the impact of agricultural activities on groundwater quality will not be visible for many decades for layers thicker than 10 m. Due to the large buffering capacity of the relatively dense unsaturated layer, there has been an amplitude shift of up to hundreds of years between land-use changes and the groundwater quality response (Huang et al. 2013). Therefore, the Cenomanian–Turonian formations represent 69% of the outcrop in the Meskala-Ouazzi (Laftouhi et al. 2003).

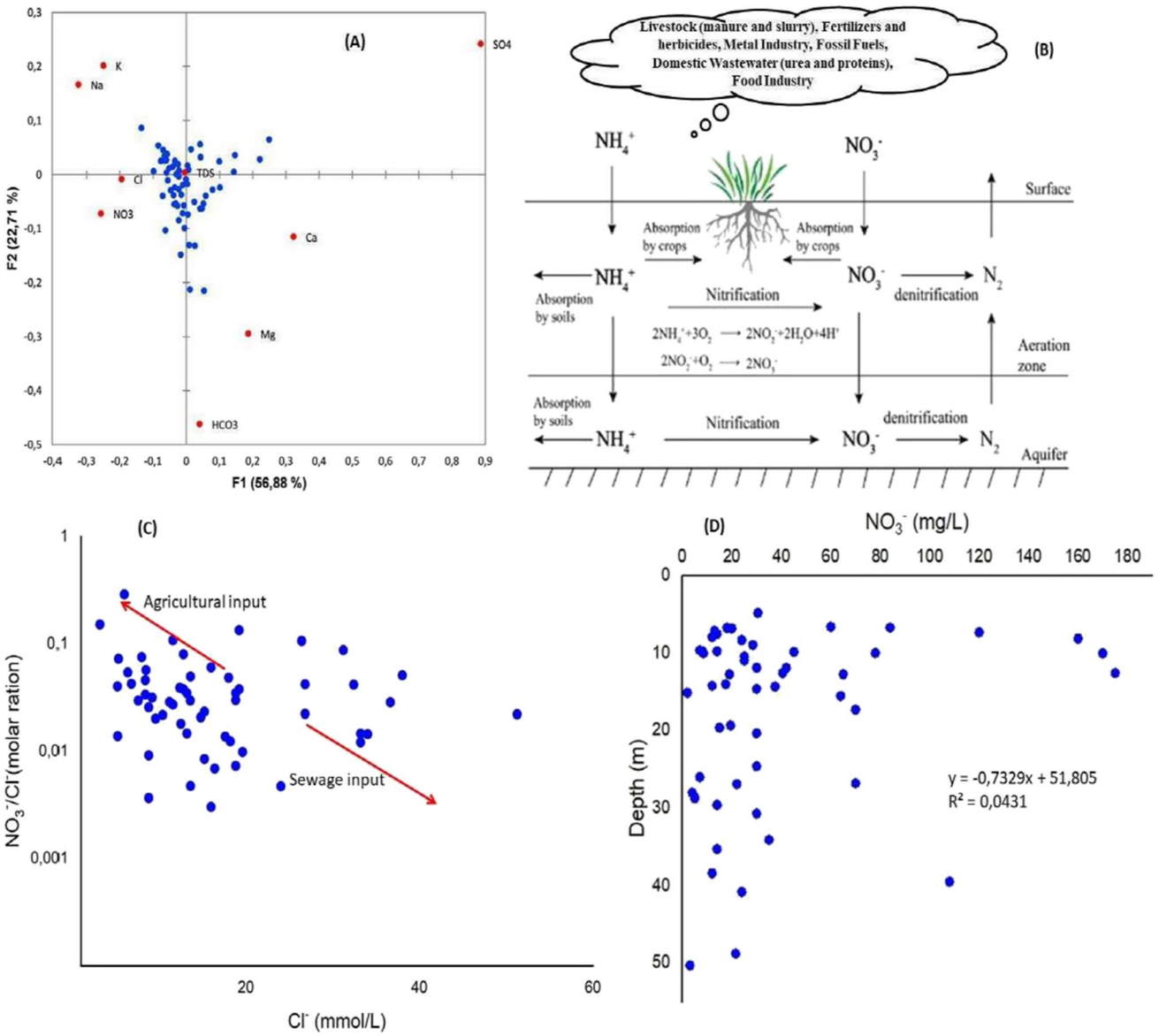

Fig. 5 **A** CA plane plots of study area, **B** nitrogen cycle (modified after Wei et al., 2017), **C** variations in NO_3^-/Cl^- molar concentrations, and **D** plot of NO_3^- concentrations versus depth of groundwater

Table 4 Coordinate data of parameters from correspondence analysis of Meskala-Ouazi sub-basin

Parameters	Factor loadings	
	F1	F2
TDS	−0.005	0.004
Ca^{2+}	0.323	−0.115
Mg^{2+}	0.187	−0.295
Na^+	−0.324	0.166
K^+	−0.249	0.201
HCO_3^-	0.041	−0.462
Cl^-	−0.194	−0.008
SO_4^{2-}	0.887	0.242
NO_3^-	−0.257	−0.073

A multi-layered aquifer in the Meskala-Ouazzi sub-basin is contained in fractured and karstic materials (Bahir et al. 2000). In certain areas, these thin soils are in close touch with the karst aquifer, and fertilizers are directly transferred to groundwater from the unsaturated layer (El Mountassir et al. 2021a). Therefore, it seemed inappropriate to explain the elevated concentrations relative to groundwater levels in terms of thickness in coastal aquifers.

Potential NO_3^- pollution path

The nitrate concentrations ranged from 2 to 175 mg/L (Table 5) (Fig. 6a), with 22.41% of the water samples above

Table 5 Descriptive analysis of nitrate (mg/L), nitrate pollution index (NPI), and groundwater pollution index (GPI) in the study area

Parameter	Min	Max	Mean	SD	CV
NO_3^- (mg/L)	2	175	37.5	39.95	1.07
NPI	−0.9	7.8	0.9	2	2.29
GPI	0.56	3.66	1.68	0.78	0.46

the WHO guidelines for drinking water quality (50 mg/L) (WHO 2011) and 82.75% below the drinking water quality standards (Fig. 6b). The highest concentrations of nitrate were found in southwestern and in the center of the study area (Fig. 6a), with the highest concentrations at points S5, S11, S12, S15, S18, S35, S38, S46, and S47.

These highest concentrations could be explained by:

All wells with nitrate contents above the threshold of 50 mg/L are generally located next to cemeteries and this to have access to water for post-mortem ablutions. We believe that a significant amount of nitrates come from the degradation of the remains.

A second potential agent for contamination of groundwater in the Meskala-Ouazzi region by nitrates consists in poor protection of wells and especially against the permanent puddles surrounding the structures which are heavily loaded with excrement from animals coming for watering and also for the water supply of the inhabitants (Mennani et al. 2001b). The extremely fractured character of the limestones and dolomitic limestones of the Cenemano-Turonian aquifer, as well as the thinness of the unsaturated zone, means that the pollutant flow can easily reach the groundwater by percolation. In fact, nitrates are practically not retained in the soil (behavior of a tracer with little ion exchange) and therefore easily reach the groundwater (Sall and Vanclooster 2009). The transformation of nitrogenous elements takes place in the unsaturated zone (Banton et al. 1995) to result in nitrates which are very mobile. This type of pollution is very frequent in the countries of West Africa (Mudry and Travi 1992).

The third potential factor for this nitrate contamination corresponds to the absence of a sanitation network allowing the evacuation of wastewater. This means that people are faced with the obligation to use septic tanks which represent a danger for groundwater, for example, well S38 which is near the village of Krimat and which recorded a very high value of 175 mg/L. The second well is S15 which is near the village of Meskala east which registers a very high value of nitrate concentration with 160 mg/L.

The fourth factor is that of slaughterhouses such as the rural supermarkets plus the slaughterhouse waste (more than 150 heads slaughtered every Monday) is accumulated just upstream of the few wells that have recorded high values of nitrates.

The fifth factor is that of the tourist effect; this is the case of well S46 which is very close to the Atlantic Ocean; this well is recorded a very strong value of 170 mg/L.

Finally, the last factor seems ineffective, even if it is usually the classic agent of nitrate pollution; it is the use of fertilizers. Indeed, in the region studied and in the absence of developed agriculture, agricultural fertilizers and soil improvers are very little used. However, their contribution to nitrates in groundwater should not be overlooked.

Diffuse nitrate contamination is a result of several factors (lhadi et al. 1996), which are the nature of the soil, the rainfall, the lithology and permeability of the aquifer, and the depth of the water table.

The NPI ranged between −0.9 and 7.8 (Table 5). According to the classification of NPI, 44.8% of the total groundwater samples represent clean water, 29.3% light pollution, 6.9% moderate pollution, 8.6% significant pollution, and the remaining 10.4% very significant pollution.

The lowest values of NPI relative to clean water in terms of anthropogenic nitrate are found in all areas of the Meskala-Ouazzi sub-basin, according to the spatial distribution of NPI shown in Fig. 6c. Based on NPI values, light nitrate pollution dominates the majority of the region, particularly from north to south and east to west of central areas. The NPI values revealed that anthropogenic nitrate pollution is most prevalent in the central region at medium, high, and very significant levels, characterized by agriculture, and for the downstream region, it is a tourist region. In this way, these areas contain high nitrate values.

Pollution index groundwater (PIG)

In this case study, the pollution index groundwater (PIG) values range from 0.56 to 3.66 (Table 5) (Fig. 6d). PIG classifies 13.8% of overall groundwater samples as "insignificant pollution," 37.9% as "low pollution," 20.7% as "medium pollution," 8.6% as "high pollution," and the remaining 19% as "extremely high pollution."

The spatial distribution of zones of PIG is depicted in Fig. 6d. Insignificant pollution and low pollution zone are observed from the upstream zone in the Cenemano-Turonian aquifer exactly in the Bouabout region which is characterized by the groundwater recharge zone (El Mountassir et al. 2021a). Moderate pollution zone was observed throughout the study area except for the aquifer recharge area. High pollution and very high pollution zone are recorded in the central and the downstream part of the study area part, which is characterized by strong urbanization like villages Meskala and Krimat; on the other hand, the second zone is a tourist zone like the village of Sidi Kaouki which does not contain a sewerage network and therefore the infiltration of pollution on the water table quickly. Thus, the spatial distribution of zones of PIG is increased gradually from upstream to

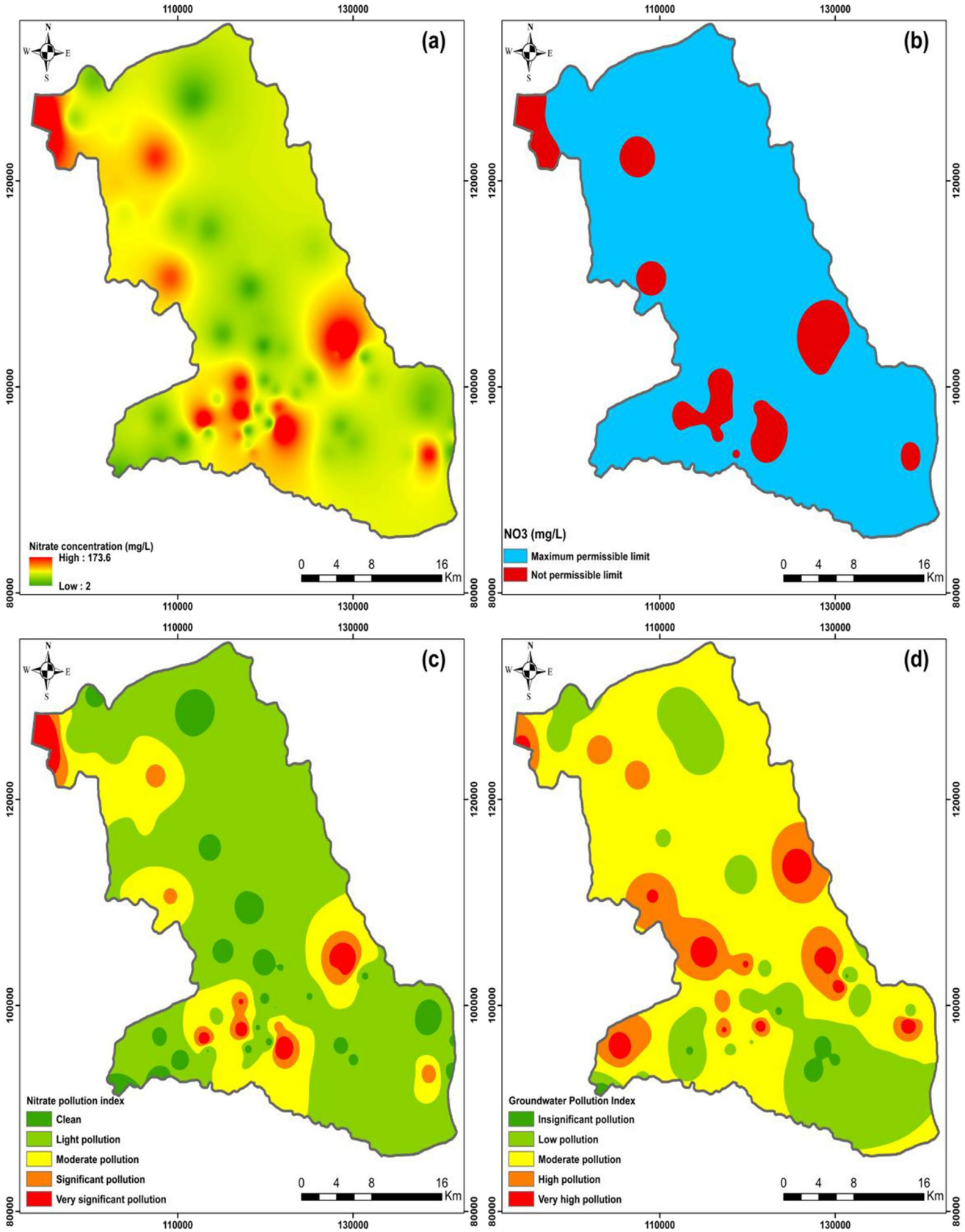

Fig. 6 **a** Spatial map of nitrate distribution in the study area; **b** spatial distribution map of nitrate based in WHO 2011; **c** spatial distribution map of nitrate pollution index (NPI); **d** distribution of groundwater quality based on groundwater pollution index (GPI)

downstream. This means that a combination of values for different concentrations of water quality controls led to a gradual rise in pollution from an insignificant level to a very high level pollution.

Tritium (δ^3H)

The tritium contents in the Meskala-Ouazzi sub-basin groundwater samples vary between 0 and 2.1 TU with a mean of 0.67 (Table 6). As shown on the diagram (Fig. 7a), only four groundwater samples indicate significant values of tritium greater than 1 TU.

Tritium content greater than 1 TU indicates post-nuclear water recharge, whereas content less than 1 TU indicates pre-nuclear water recharge or mixing of modern and ancient waters, according to Mazor (1991). Indeed, high tritium contents were observed downstream of the study area (Fig. 7b) which is characterized by the discharge of the aquifer and can be attributed to recent precipitation infiltration. The recharge of aquifers is mainly associated with the direct infiltration of recent rainwater of Atlantic Oceanic origin which shows the vulnerability of this aquifer to any contamination (El Mountassir et al. 2021a).

The high δ^3H contents confirm the modern infiltration of recent waters (post-1952) in the Meskala-Ouazzi sub-basin, particularly in the shallow aquifer. More than 78% of groundwater samples show low tritium values (i.e., less than 1 TU). This indicates either the ancient origin of the waters or the existence of a mixing phenomenon between recent and old waters (Fig. 7c).

The variation of tritium contents in groundwater samples according to NO_3^- (Fig. 7d) concentrations indicate that samples with high nitrate contents greater than 50 mg/L (World health organization limit for drinking water) (WHO 2011) also contain significant tritium values ($\delta^3H > 1$ UT) (Fig. 7d), especially for the samples N° E1, N° E10, and N° E18. This could be explained by the recent origin of nitrate contamination proving the contribution of return flow of irrigation water, enriched in nitrate fertilizers, to aquifer recharge (Kammoun et al. 2021). Furthermore, the high value of nitrates in some places can be explained by its presence in a residential area, due to the lack of a sanitation network in the village.

However, the generalized decrease in the H content could be explained by the low recharge rate following the decrease in the precipitation rate due to climate change (Chabour et al. 2021; El Mountassir et al. 2021a,b,c).

Conclusions

In recent years, overexploitation of fertilizers has become a threat to groundwater quality due to the leakage of nitrates into the aquifer. Based on 58 groundwater samples in the Essaouira region, a correspondence analysis, a groundwater pollution index, a stoichiometric analysis, main ion ratios, a nitrate pollution index, and an analysis qualitative are used

Table 6 Isotopic composition of analyzed samples in Meskala-Ouazzi sub-basin

Sample	pH	T °C	TDS mg/L	NO_3^- mg/L	$\delta^{18}O$ (‰ vs. SMOW)	δ^3H (TU)
E1	7.49	19.5	1408.51	78.75	−4.83	1.5
E2	7.63	21	718.18	32.25	−5.16	0.8
E3	7.37	19.2	781.30	29.14	−5.73	0.7
E4	7.23	22.1	692.09	42.79	−5.52	0
E5	7.31	19.8	414.82	80.61	−4.63	0.6
E6	7.11	18.5	1384.69	127.12	−4.89	0.7
E7	7.23	18	1700.49	96.12	−3.28	0
E8	7.03	22.1	2531.71	0	−6.01	0.5
E9	6.91	23.7	1108.18	19.84	−5.5	0.2
E10	6.87	20.9	913.20	97.98	−5.06	2.1
E11	6.99	23	2212.33	113.48	−4.61	0.6
E12	7.15	23.3	993.25	0	−4.34	1.2
E13	7.07	21.2	1060.98	66.35	−4.88	0.7
E14	6.99	23.4	1810.59	35.97	−5.35	0.2
E15	7.04	22.1	990.53	0	−4.58	0.7
E16	7.33	24	1383.13	60.15	−5.08	0
E17	6.99	23.2	1776.13	61.39	−5	0.7
E18	7.32	19.6	1713.20	70.07	−4.63	1
E19	7.11	20.5	2519.27	391.28	−3.9	0.6

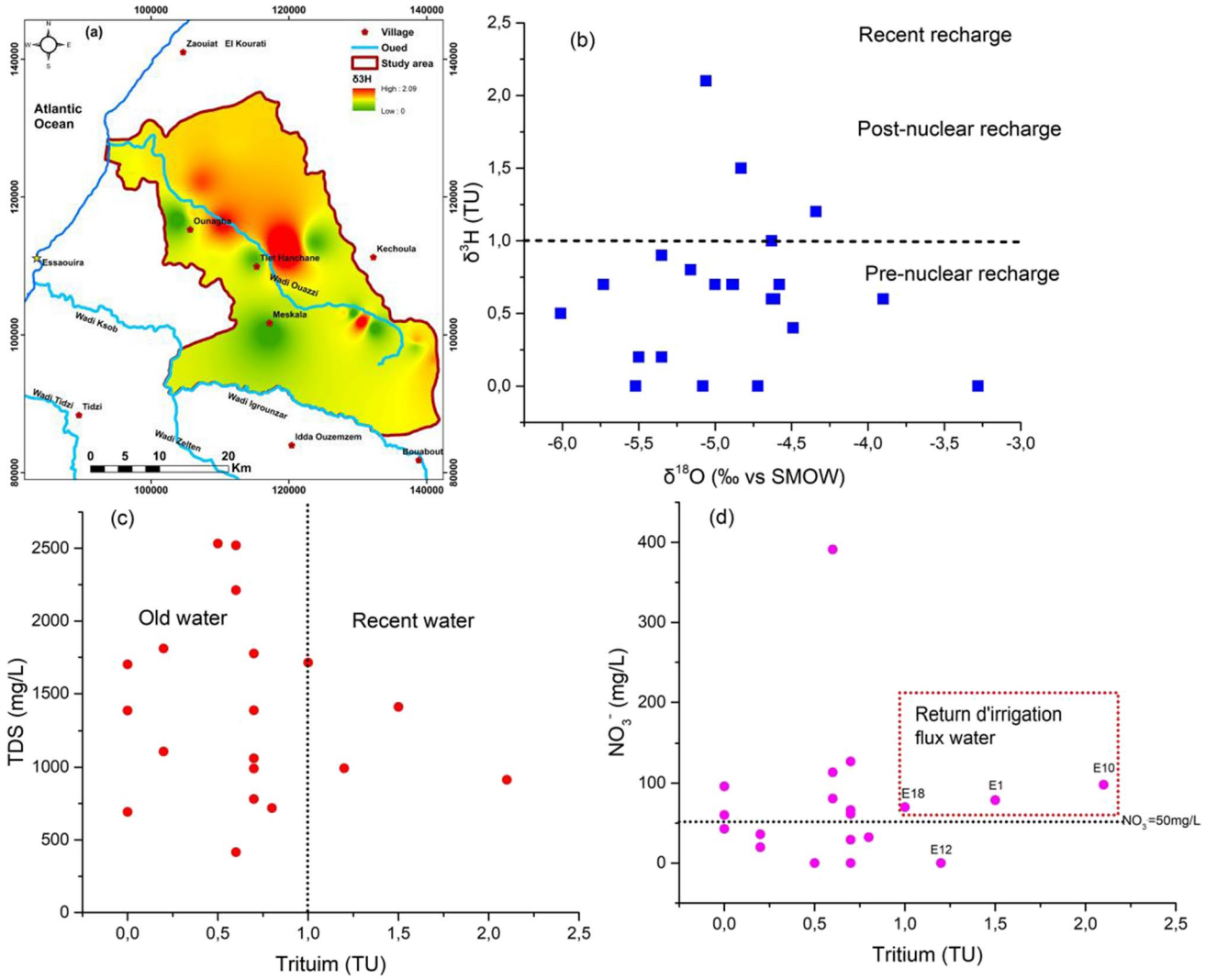

Fig.7 **a** Spatial distribution of tritium (δ^3H), **b** radioactive isotope δ^3H versus δ^2O (‰ vs SMOW), **c** TDS vs tritium, **d** nitrate vs tritium in the Meskala-Ouazi sub-basin

to systematically discuss the spatial heterogeneity of nitrate concentrations and possible pollution pathways.

The chemical facies in the study area reveals that the Cenomanian–Turonian groundwater is of the types Ca–Mg–Cl and Ca-SO4, with the first type dominating. For all the groundwater samples, chloride (Cl^-) was the dominant anion and calcium (Ca^{2+}) was the dominant cation. As a result, an examination of physical parameters (pH and electrical conductivity (EC)) reveals that groundwater is neutral, with a high level of mineralization. Indeed, 90% of the samples examined had EC values greater than 1500 s/cm, indicating low performance.

The ACP suggested that two main components could explain 79.59% of the total variance of 9 physical–chemical parameters, indicating that the hydrogeochemical evolution of groundwater was mainly controlled by gypsum and halites, cation exchange, the dissolution/precipitation of carbonates, and anthropogenic activities.

The recharge of aquifers is mainly associated with the direct infiltration of recent rainwater, the return of irrigation water, and in small part with artificial recharge. In particular, in the center of the study area, the impact of the infiltration of irrigated water on the recharge of the aquifer is very important. For the study area, it reveals the existence of two recharging periods: the pre-nuclear and post-nuclear, depending on the concentrations of tritium. The results of this work will help the administration, decision-makers, and the general public to understand the state of groundwater pollution, as well as to monitor and manage the water supplies of the Meskala-Ouazzi sub-basin in order to minimize the effects potentials on human health.

Acknowledgements We thank the editor-in-chief Dr. Philippe Garrigues, editor Dr. Xianliang Yiand, and the reviewers for their critical reviews and valuable suggestions. Special thanks go to people from the National Office of drinking water (ONEE) at the Essaouira city for their assistance; we thank The Pr. EBN TOUHAMI Mohamed dean of the Faculty of Sciences of Kenitra, for his assistance during the chemical analyses of K and Na of the campaign 2019. The authors are grateful to our colleagues for their assistance in data collection and field investigation. I dedicate this article to my father who passed away the past two months Mr. Abdellatif el Mountassir who for many years sacrificed everything he had to help me move forward in my scientific research and in life. May God grant this work to bear fruit. I thank him for all the noble values, education, and support that came from him.

Author contributions Conceptualization: O.E.M., M.B.; methodology: O.E.M; software, O.E.M.; validation: O.E.M., M.B., A.C., D.O, and P.M.C; formal analysis and investigation: O.E.M., M.O.; resources: O.E.M., M.B, and P.M.C; writing—original draft preparation: O.E.M.; writing—review and editing: O.E.M., M.B; visualization: O.E.M., M.B., A.C., D.O, and P.M.C; supervision: M.B; project administration: M.B; all authors have read and agreed to the published version of the manuscript.

Data availability All data generated or analyzed during this study are included in this published article.

Declarations

Ethical approval and consent to participate This manuscript does not contain any individual person's data and ethics approval is not required.

Consent for publication Not applicable.

Conflict of interest The authors declare no competing interests.

References

Angers B, Magnan P, Plante M, Bernatchez L (1999) Canonical correspondence analysis for estimating spatial and environmental effects on microsatellite gene diversity in brook charr (Salvelinus fontinalis). Mol Ecol 8:1043–1053

Appelo C.A.J, Postma D (2014) Geochemistry, groundwater and pollution. CRC press.

Assaf H, Saadeh M (2009) Geostatistical assessment of groundwater nitrate contamination with reflection on DRASTIC vulnerability assessment: the case of the Upper Litani Basin. Lebanon Water Resour Manag 23(4):775–796. https://doi.org/10.1007/s11269-008-9299-8

Axinte O, Bădescu IS, Stroe C, Neacsu V, Bulgariu L, Bulgariu D (2015) Evolution of trophic parameters from Amara Lake. Environ Eng Manag J 14:559–565

Axinte O, Volf I, Bulgariu L (2017) Adaptive management for sustainable development of Amara Lake (SE Romania). Environ Eng Manag J 16:625–631

Bahir M, Mennani A, Jalal M, Youbi N (2000) Ressources hydriques du bassin synclinal d'Essaouira (Maroc). Estudios Geologicos 56:185–195

Bahir M, El Moukhayar R, Chamchati H, Youbi N, Carreira PM, Chkir N (2014) Recharge and hydrogeochemical evolution groundwater in semi-arid zone (Essaouira Basin, Morocco). Comun Geol J 101:651–653

Bahir M, Ouazar D, Ouhamdouch S (2018) Characterization of mechanisms and processes controlling groundwater salinization in coastal semi-arid area using hydrochemical and isotopic investigations (Essaouira basin, Morocco). Environ Sci Pollut Res 25:24992–25004. https://doi.org/10.1007/s11356-018-2543-8

Bahir M, El Mountassir O, Ouazar D, Carreira P.M (2021a) Hydrochemical analysis and evaluation of groundwater quality in Ouazi Basin (Essaouira, Morocco). In: Abrunhosa M., Chambel A., Peppoloni S., Chaminé H.I. (eds) Advances in geoethics and groundwater management: theory and practice for a sustainable development. Advances in Science, Technology & Innovation (IEREK Interdisciplinary Series for Sustainable Development). Springer, Cham. https://doi.org/10.1007/978-3-030-59320-9_50

Bahir M, El Mountassir O, Ouazar D, Carreira P.M (2021b) Use of WQI and isotopes to assess groundwater quality of coastal aquifers (Essaouira, Morocco). In: Abrunhosa M., Chambel A., Peppoloni S., Chaminé H.I. (eds) Advances in geoethics and groundwater management: theory and practice for a sustainable development. Advances in Science, Technology & Innovation (IEREK Interdisciplinary Series for Sustainable Development). Springer, Cham. https://doi.org/10.1007/978-3-030-59320-9_51

Bahrami M, Zarei AR, Rostami F (2020) Temporal and spatial assessment of groundwater contamination with nitrate by nitrate pollution index (NPI) and GIS (case study: Fasarud Plain, southern Iran). Environ Geochem Health 42:3119–3130. https://doi.org/10.1007/s10653-020-00546-x

Banton O, Laroque M, Cormier M (1995) Modélisation du transport des nitrates dans la zone non saturée pour l'évaluation de la contamination des eaux souterraines. Hydrogeologie 4:23–30

Barkat A, Bouaicha F, Bouteraa O, Mester T, Ata B, Balla D, Rahal Z, Szabó G (2021) Assessment of complex terminal groundwater aquifer for different use of Oued Souf Valley (Algeria) using multivariate statistical methods, geostatistical modeling, and water quality index. Water 13(11):1609. https://doi.org/10.3390/w13111609

Bouaicha F, Dib H, Bouteraa O, Manchar N, Boufaa K, Chabour N, Demdoum A (2019) Geochemical assessment, mixing behavior and environmental impact of thermal waters in the Guelma geothermal system, Algeria. Acta Geochim 38:683–702. https://doi.org/10.1007/s11631-019-00324-2

Bouteraa O, Mebarki A, Bouaicha F, Nouaceur Z, Laignel B (2019) Groundwater quality assessment using multivariate analysis, geostatistical modeling, and water quality index (WQI): a case of study in the Boumerzoug-El Khroub valley of Northeast Algeria. Acta Geochimica 38(6):796–814. https://doi.org/10.1007/s11631-019-00329-x

Brindha K, Vaman KN, Srinivasan K, Babu MS, Elango L (2014) Identification of surface water-groundwater interaction by hydrogeochemical indicators and assessing its suitability for drinking and irrigational purposes in Chennai. Southern India Appl Water Sci 4:159–174. https://doi.org/10.1007/s13201-013-0138-6

Carreira PM, Bahir M, Ouhamdouch S, Galego Fernandes P, Nunes D (2018) Tracing salinization processes in coastal aquifers using an isotopic and geochemical approach: comparative studies in western Morocco and southwest Portugal. Hydrogeol J 26:2595–2615. https://doi.org/10.1007/s10040-018-1815-1

Castany G (1982) Principes et Méthodes de l'Hydrogéologie (2ème édn). Collection Dunod Université-Bordas, Paris

Chabour N, Dib H, Bouaicha F, Bechkit MA, Nacer NM (2021) A conceptual framework of groundwater flowpath and recharge in Ziban aquifer: south of Algeria. Sustain Water Resour Manag 7:1–15. https://doi.org/10.1007/s40899-020-00483-8

Duffaud F (1960) Contribution à l'étude stratigraphique du bassin secondaire du Haut Atlas Occidental (Sud-Ouest du Maroc). Bull Soc Géol Fr 7:728–734. https://doi.org/10.2113/gssgfbull.S7-II.6.728

Elango L, Kannan R (2007) Rock–water interaction and its control on chemical composition of groundwater. Devts Environ Sci 5:229–243. https://doi.org/10.1016/S1474-8177(07)05011-5

El Mountassir O, Bahir M, Ouazar D, Ouhamdouch S, Chehbouni A, Ouarani M (2020) The use of GIS and water quality index to assess groundwater quality of krimat aquifer (Essaouira; Morocco). SN Appl Sci 2:881. https://doi.org/10.1007/s42452-020-2653-z

El Mountassir O, Ouazar D, Bahir M, Chehbouni A, Carreira PM (2021a) GIS-based assessment of aquifer vulnerability using DRASTIC model and stable isotope: a case study on Essaouira basin. Arab J Geosci 14:1–21. https://doi.org/10.1007/s12517-021-06540-6

El Mountassir O, Bahir M, Ouazar D, Carreira P.M. (2021b) For a better understanding of recharge and salinization mechanism of a Cenomanian–Turonian aquifer. In: Abrunhosa M., Chambel A., Peppoloni S., Chaminé H.I. (eds) Advances in geoethics and groundwater management: theory and practice for a sustainable development. Advances in Science, Technology & Innovation (IEREK Interdisciplinary Series for Sustainable Development). Springer, Cham. https://doi.org/10.1007/978-3-030-59320-9_42

El Mountassir O, Bahir M, Ouazar D, Chehbouni A, Carreira PM (2021c) Geochemical and isotopic evidence of groundwater salinization processes in the Essaouira region, north-west coast, Morocco. SN Appl Sci 3:1–16. https://doi.org/10.1007/s42452-021-04623-3

Fenandes GP, Bahir M, Mendonça J, Carreira P, Fakir Y, Silva MO (2005) Anthropogenic features within Sines (Portugal) and Essaouira (Morocco) coastalaquifers by PCA-hydrochemical evolution comparative study. Estudios Geol 61:207–219

Filintas A (2005) Land use systems with emphasis on agricultural machinery, irrigation and nitrates pollution, with the use of satellite remote sensing, geographic information systems and models, in watershed level in Central Greece. M.Sc. thesis, Dept. of Environment, University of Aegean, Mitilini, Greece

Hamed Y, Hadji R, Redhaounia B, Zighmi K, Bâali F, El Gayar A (2018) Climate impact on surface and groundwater in North Africa: a global synthesis of findings and recommendations. Euro-Mediterr J Environ Integr 3:25. https://doi.org/10.1007/s41207-018-0067-8

Han ZJ, Jin ZS (1996) Hydrology of Guizhou Province. Seismology Press Beijing, China

Huang T, Pang Z, Yuan L (2013) Nitrate in groundwater and the unsaturated zone in (semi)arid northern China: baseline and factors controlling its transport and fate. Environ Earth Sci 70:145–156. https://doi.org/10.1007/s12665-012-2111-3

Ji X, Xie R, Hao Y, Lu J (2017) Quantitative identification of nitrate pollution sources and uncertainty analysis based on dual isotope approach in an agricultural watershed. Environ Pollut 229:586–594. https://doi.org/10.1016/j.envpol.2017.06.100

Kaid Rassou K, Fakir Y, Bahir M, Zouari K, Marah M (2005) Origine et datation des eaux Souterraines du sahel d'Eloualidia. Estudios Geol 61:191–196

Kamaraj J, Sekar S, Roy PD, Senapathi V, Chung SY, Perumal M, Nath AV (2021) Groundwater pollution index (GPI) and GIS-based appraisal of groundwater quality for drinking and irrigation in coastal aquifers of Tiruchendur, South India. Environ Sci Pollut Res 6:1–9. https://doi.org/10.1007/s11356-021-12702-6

Kammoun S, Trabelsi R, Re V, Zouari K (2021) Coastal aquifer salinization in semi-arid regions: The case of Grombalia (Tunisia). Water 13:129. https://doi.org/10.3390/w13020129

Karami S, Madani H, Katibeh H, Marj AF (2018) Assessment and modeling of the groundwater hydrogeochemical quality parameters via geostatistical approaches. Appl Water Sci 8(1):1–3. https://doi.org/10.1007/s13201-018-0641-x

Laftouhi NE, Vanclooster M, Jalal M, Witam O, Aboufirassi M, Bahir M, Persoons É (2003) Groundwater nitrate pollution in the Essaouira Basin (Morocco). Comptes Rendus - Geoscience 335:307–317. https://doi.org/10.1016/S1631-0713(03)00025-7

Lark RM (2000) Estimating variograms of soil properties by the method-of-moments and maximum likelihood. Eur J Soil Sci 51:717–728

Lhadi EK, Mountadar M, Younsi A, Martin G, Morvan J (1996) Pollution par les nitrates des eaux souterraines de la zone littorale de la province d'el Jadida (Maroc). Hydrogéologie 3:35–49

Lucas LL, Unterweger MP (2000) Comprehensive review and critical evaluation of the half-life of tritium. J Res Natl Inst Stand Technol 105:541. https://doi.org/10.6028/jres.105.043

Mazor E (1991) Applied chemical and isotopic groundwater hydrology. Open University Press, Buckingham

Mei K, Liao L, Zhu Y, Lu P, Wang Z, Dahlgren RA, Zhang M (2014) Evaluation of spatial-temporal variations and trends in surface water quality across a rural-suburban-urban interface. Environ Sci Pollut Res 21:8036–8051

Mekala C, Gaonkar O, Nambi IM (2017) Understanding nitrogen and carbon biogeotransformations and transport dynamics in saturated soil columns. Geoderma 285:185–194. https://doi.org/10.1016/j.geoderma.2016.10.004

Mennani A (2001a) Apport de l'hydrochimie et de l'isotopie à la connaissance du fonctionnement des aquifères de la zone côtière d'Essaouira (Maroc Occidental). PhD Thesis, Cadi Ayyad University, Marrakech, Morocco

Mennani A, Blavoux B, Bahir M, Bellion Y, Jalal M, Daniel M (2001) Apports des analyses chimiques et isotopiques a la connaissance du fonctionnement des aquiferes plio-quaternaire et turonien de la zone synclinale d'Essaouira. Maroc Occidental J Afr Earth Sci 32:819–835. https://doi.org/10.1016/S0899-5362(02)00057-X

Mtoni Y, Mjemah IC, Bakundukize C, Van Camp M, Martens K, Walraevens K (2013) Saltwater intrusion and nitrate pollution in the coastal aquifer of Dar es Salaam, Tanzania. Environ Earth Sci 70:1091–1111. https://doi.org/10.1007/s12665-012-2197-7

Mudry J, Travi Y (1992) Evaluation du 'risque nitrate' dans les aquifères de socle de l'afrique de l'ouest. Revue de la faculté des sciences semlalia Marrakech. p 171–174

Nejatijahromi Z, Nassery HR, Hosono T, Nakhaei M, Alijani F, Okumura A (2019) Groundwater nitrate contamination in an area using urban wastewaters for agricultural irrigation under arid climate condition, southeast of Tehran. Iran Agric Water Manag 221:397–414. https://doi.org/10.1016/j.agwat.2019.04.015

Obeidat MM, Massadeh AM, Al-Ajlouni AM, Athamneh FS (2007) Analysis and evaluation of nitrate levels in groundwater at Al-Hashimiya area. Jordan Environ Monit Assess 135:475–486. https://doi.org/10.1007/s10661-007-9667-5

Obeidat M. M, Al-Ajlouni A, Al-Rub F. A, Awawdeh M (2012) An innovative nitrate pollution index and multivariate statistical investigations of groundwater chemical quality of Umm Rijam Aquifer (B4), North Yarmouk River Basin, Jordan," Chapters, in: Konstantinos (Kostas)

Panno SV, Hackley KC, Hwang HH, Kelly WR (2001) Determination of the sources of nitrate contamination in karst springs using isotopic and chemical indicators. Chem Geol 179:113–128. https://doi.org/10.1016/S0009-2541(01)00318-7

Redwan M, Moneim A. A. A, Mohammed N. E, Masoud A. M (2020) Sources and health risk assessments of nitrate in groundwater, West of Tahta area, Sohag, Egypt. Episodes 1:1–10. https://doi.org/10.18814/epiiugs/2020/020048

Sall M, Vanclooster M (2009) Assessing the well water pollution problem by nitrates in the small scale farming systems of the Niayes region, Senegal. Agric Water Manag 96:1360–1368. https://doi.org/10.1016/j.agwat.2009.04.010

Seo Y, Kim S, Singh VP (2015) Estimating spatial precipitation using regression kriging and artificial neural network residual kriging

(RKNNRK) hybrid approach. Water Resour Manag 29:2189–2204. https://doi.org/10.1007/s11269-015-0935-9

Subba Rao N (2012) PIG: a numerical index for dissemination of groundwater contamination zones. Hydrol Process 26:3344–3350. https://doi.org/10.1002/hyp.8456

Trabelsi R, Zouari K (2019) Coupled geochemical modeling and multivariate statistical analysis approach for the assessment of groundwater quality in irrigated areas: a study from North Eastern of Tunisia. Groundw Sustain Dev 8:413–427. https://doi.org/10.1016/j.gsd.2019.01.006

Venkatramanan S, Chung SY, Kim TH, Kim BW, Selvam S (2016) Geostatistical techniques to evaluate groundwater contamination and its sources in Miryang City. Korea Environ Earth Sci 75:994. https://doi.org/10.1007/s12665-016-5813-0

Wei YN, Fan W, Wang W, Deng L (2017) Identification of nitrate pollution sources of groundwater and analysis of potential pollution paths in loess regions: a case study in Tongchuan region. China Environ Earth Sci 76:423. https://doi.org/10.1007/s12665-017-6756-9

WHO (2011) Guidelines for drinking-water quality, 4th edn. Geneva, Switzerland, WHO Press

Wu J, Li P, Qian H, Duan Z, Zhang X (2014) Using correlation and multivariate statistical analysis to identify hydrogeochemical processes affecting the major ion chemistry of waters: a case study in Laoheba phosphorite mine in Sichuan, China. Arab J Geosci 7:3973–3982. https://doi.org/10.1007/s12517-013-1057-4

Wu J, Sun Z (2016) Evaluation of shallow groundwater contamination and associated human health risk in an alluvial plain impacted by agricultural and industrial activities, Mid-west China. Expo Health 8:311–329. https://doi.org/10.1007/s12403-015-0170-x

Yuan J, Xu F, Deng G, Tang Y, Li P (2017) Hydrogeochemistry of shallow groundwater in a karst aquifer system of Bijie city. Guizhou Province Water 9:625. https://doi.org/10.3390/w9080625